THE PENNSYLVANIA STATE UNIVERSITY
SCHREYER HONORS COLLEGE

DEPARTMENT OF BIOMEDICAL ENGINEERING

THE ROLE OF MECHANICALLY GATED ION CHANNELS IN REGULATING THE RESPONSE OF MESENCHYMAL STEM CELLS TO NANOFIBER ARCHITECTURE

GRANT D WANDLING
SPRING 2018

A thesis
submitted in partial fulfillment
of the requirements
for a baccalaureate degree
in Biomedical Engineering
with honors in Biomedical Engineering

Reviewed and approved* by the following:

Justin L. Brown
Associate Professor of Biomedical Engineering
Thesis Supervisor

William Hancock
Professor of Biomedical Engineering
Honors Adviser

Daniel Hayes
Associate Professor of Biomedical Engineering
Reader

* Signatures are on file in the Schreyer Honors College.

ABSTRACT

The human body is a constantly changing, heterogeneous structure often in need of assistance in times of trauma and aging. Over one hundred billion dollars are spent on orthopedic trauma, malignancy, infection, and degradation care and repair. Many of these cases require intervention to achieve and maintain union between healing bone components, which is needed by bone cells to properly correct the injured site.

The living cells within the human body must perceive and react to their surroundings in order to carry out their basic functions and repair damaged tissues. The physical interaction between a cell and the extracellular matrix is a complex structure and process comprised of many protein interactions. A cell uses these interactions to interpret and respond to the changes in their surroundings, often by converting a physical force into an electrochemical signal.

These signals are sometimes created by the movement of ions across a membrane, through a transmembrane channel. TREK-1 is a transmembrane potassium channel responsible for maintaining the cell membrane potential. We hypothesize that changes in the extracellular architecture will alter the expression of TREK-1. Alterations of the extracellular geometry will lead to changes in the forces applied to cells, eliciting an electrochemical response, which must be regulated by ion channels such as TREK-1.

By using techniques such as western blotting, ELISA, and immunofluorescence imaging, we can detect concentrations of TREK-1 in osteoblast and human mesenchymal stem cells. While no trend was observed due to low protein concentrations, the presence of TREK-1 was verified in multiple cell lines. Future work in this area will look to expand the variety of extracellular architectures and better quantify protein expression levels on these substrates.

TABLE OF CONTENTS

LIST OF FIGURES

ACKNOWLEDGEMENTS

While so many people helped me reach this point in my academic life, and I wish I could thank each one individually, I would like to take the time to acknowledge several key individuals whose assistance and guidance made a meaningful impact on my path.

First, I would like to thank Dr. Justin Brown for his advice and assistance with my project, in addition to teaching us all something about good cars, coffee, and beer. I would also like to thank the rest of my thesis committee for their time and advice during my project. Second, I would not have made any progress in the lab without the assistance of Brittany Banik, Dan Bowers, or Pouria Fattahi and they deserve my utmost thanks and appreciation. Brittany took the time to teach me almost everything I know in the lab and without her this work would have been a great deal more difficult. I would also like to thank my previous professors and instructors from elementary, middle, high school, and college for all they have taught me.

Additionally, I must thank my friends for their support and encouragement. College and thesis work without my teammates and players to help me relax would certainly have been more stressful. To paraphrase Shakespeare, “He who sheds his blood with me, shall be my brother”. Spending time in good company is always important and somehow, I managed to find only the best. The hours spent amongst this group of friends will forever be some of my most cherished memories.

Lastly, my family deserves my undying gratitude and thanks. My parents worked tirelessly to make sure I have everything I need to succeed, including their love and support. Without their help, I would not have been able to accomplish even the smallest tasks. Everything they’ve done to help me along the way means the world to me and I know I can never repay them. I only hope they know how much I appreciate everything they’ve done.

Chapter 1

Introduction

1.1 Biology and Clinical Need

Bone is an important and dynamic tissue within the body, responsible for locomotion, protection of vital organs, ion and electrolyte homeostasis, and hematopoiesis.[1] On a macroscopic level bone can be divided into two groups; cortical and trabecular. Varying from bone-to-bone, the adult human skeleton consists of 80% cortical bone and 20% cancellous bone.[2] Cortical bone is hard and dense, surrounding the soft spongy cancellous bone inside and providing the mechanical support to the body necessary for locomotion and protection.[1,3] Cortical bone is comprised of osteons, organizations of bone cells.[4] Cortical osteons form 200-400 mm branching cylindrical networks called Haversian systems.[1,5] Cancellous bone, also called trabecular or spongy bone, lies within the bones, underneath the cortical layer. This type of bone is more metabolically active than cortical bone, responsible for calcium ion exchange and hematopoiesis.[1] Cells in cancellous bone are organized into plates and rods called packets 50-400 mm thick.[4]

The 206 bones in the human body are formed through a highly organized and complex composite of type-I collagen, hydroxyapatite crystals, and bone cells.[3] There are four basic types of bone cells: Osteocytes, a mature bone cell, transduce physical stimuli into a biological response.[4] Osteoblasts create a extracellular matrix (ECM) of disorganized type-I collagen, then mineralize this ECM with hydroxyapatite crystals.[4] Conversely osteoclasts break down bone so

the collagen fibers can be reoriented depending on applied forces.[3] Osteogenic cells, or mesenchymal stem cells, can differentiate into these cells when required by the tissue.[4] These basic four cell types carry out the activities needed repair and regrow bone, in addition to maintaining healthy bone mass.

In the event of trauma to the musculoskeletal system, bones can fracture, disrupting the vasculature and causing a hematoma to form.[6] Fibroblasts, osteoblasts, chondroblasts work together form the fracture callus.[3] First fibroblasts enter the area and lay down type-III collagen.[7] Chondrocytes arise at the proximal side of the fracture, forming hyaline cartilage, while osteoblasts arise on the distal side to lay down type-I collagen. The cartilage is calcified to bone through a process called endochondral ossification and the bone is remodeled by osteoclasts and osteoblasts. The callus is reduced in size as collagen is reoriented and compact bone is formed.[3,6] In order for this process to occur, not only must the gap be less than 2 mm, but four conditions must be present; osteogenic cells, osteoconductive matrix, osteoinductive stimulus, and mechanical stability.[3] Without these conditions, successful callus formation and bone healing will not occur.

Annually over a hundred billion dollars are spent on the care and repair of patients with orthopedic trauma, malignancy, infection, and degeneration.[8] From these cases, approximately one million require interventional aid to achieve union between bone fragments for proper healing to occur.[2] Non-unions can be the result of poor vascularization leading to in insufficient nutrient supply, extreme damage to bone fragments, or disease.[3] Many of these patients require locking metal plates to correctly form and hold the fragments together with the proper level of stability and micro-stimulation to encourage bone cell growth.[3,4] Other, more extreme cases, may require bone grafts to form a proper union, the need for which can carry numerous problems.[8,9]

1.2 Bone Grafts

The ideal bone graft should poses four qualities: osteointegration, osteoconduction, osteoinduction, and osteogenesis.[10] Osteointegration is the ability of the material to seamlessly connect to the bone without formation of scar tissue. Osteoconduction allows for bone to grow over the graft. Osteoinduction is the ability to recruit and induce differentiation of stem cells from the surrounding tissue into the graft to become osteoblastic precursors. The properties allow the graft to be successfully implanted and integrated into the bone.

Autografts of cancellous bone, typically harvested from the iliac crest, fibula, rib, or tibia of the same patient they are to be implanted in, and are the most successful type of graft available.[9–11] This treatment is the gold standard of bone grafting since it displays all four qualities needed for an ideal bone graft, but it is not without its complications.[10] Operating time to harvest this tissue is lengthy and expensive, pushing heavy costs and recovery onto the patient.[9] As with any advanced operative procedure, there are ever-present risks associated with the action of harvesting the tissue such as infection, prolonged wound drainage, hematoma, reoperation, prolonged pain, and scaring.[12] One study found a major complication rate of 8.6% and a minor complication rate of 20.6%, with a significant increase in complications (17%) if the harvested tissue was taken from the same incision it was used in.[12]

The usefulness of the technique is also limited to the amount of tissue available, since only a certain amount of tissue can be harvested without compromising the donor site mechanics.[9] The application of these grafts is also limited by diffusion since most grafts are avascular.[9] Grafts have also been resorbed into the body after implantation, before bone formation from the surrounding tissue.[9,11] Although considered the gold standard for bone

grafting, the complication associated with autogenic grafting can outweigh the benefits. This leads researchers and clinicians to look for other possible sources of graft material.[9–12]

Allogenic bone grafts, tissue harvested from living donors or cadavers, are treated to strip the graft of any live components prior to implantation.[3] This reduces the risk of an immune response and rejection of the graft by the host cells.[3,11] Potential grafts are tested for various diseases and then deep frozen for 6 months, prior to retesting. This procedure also allows grafts from any donor to be implanted into any host, since the lack of live tissue does not require HLA tissue typing or ABO blood grouping. Allogenic bone grafts display three of the four qualities of a graft, lacking osteogenic cells.[10] This makes allogenic grafts one of the better current alternatives to autogenic bone grafts.

Although a good substitute for autogenic grafts, allogenic grafts are not without complications. Implantation of any foreign matter into the body is subject to immune response and rejection, in addition to the risk of infection and disease.[9] Bacterial infections are the most common and nearly 10% of large allogenic grafts are subject to this complication.[10] Transmission of viral infections such as hepatitis and HIV is rare, but has been reported in cases using seronegative cadaveric donor.[10] Fractures and non-unions are also common in allografts.[13] Up to 19% of allograft cases can result in a fracture, leading to prolonged medical complications.[10,13] The occurrence on non-union varies from the test to test, but radiological non-unions occur in approximately 17% of cases.[10] As a results of the complications associated with allogenic and autogenic bone grafts, research seeks to investigate a possible alternative that would eliminate the risks and limitations.

1.3 Alternate Bone Grafts

To solve the problems found in autogenic and allogenic bone grafts, tissue engineering and regenerative medicine look to use a combination of an artificial extracellular matrix, osteogenic cells, and soluble regulatory factors to induce bone formation.[14] An ideal synthetic bone graft would offer many of the same advantages as human bone grafts, while removing the dangers and limitations associated with autografts and allografts.[14] The ideal synthetic ECM contains three of the four necessary properties, osteointegration, osteoconduction, and osteoinduction, and is then seeded with osteogenic cells. This allows for a synthetic graft to obtain all four properties needed to be the ideal bone graft, without the need to harvest tissue form the donor.[10,14] A synthetic graft would eliminate or reduce supply limitations, donor scarcity, pathogen transfer, immune rejection, and bone resorption.[9,14]

Many different materials have been analyzed in the past several decades for their ability to meet basic requirements, as orthopedic tissue engineering is a quickly growing field.[1] These materials tend to fall within one of three categories of either bioactive glass, bioactive ceramic, and biological or synthetic polymers.[1,9,15] Ideally, these implants would be resorbed and replaced by natural tissue overtime using the body's processes.[1,15] Bio-ceramics and glass can react with physiological fluids to form a variety of scaffolds for tissue engineering, but they are limited by the biocompatibility.[16]

Natural and synthetic polymers are of special interest due to their vast diversity in structure and composition, in addition to their ability to be easily manufactured into an array of geometries and micro-architectures.[9,14,15] Because these abilities and characteristic can be used to tailor a scaffold to almost any chosen design, polymers have received a great deal of attention.[17] The natural polymer collagen is the main component of extracellular matrices throughout the

body, particularly in the musculoskeletal system.[14] Although 25 types of collagen have been identified, type I collagen is the most abundant.[17] Natural polymers like collagen have the benefit of optimal cell recognition, but are subject to impurities, cause immune responses, and inconsistency in mechanical properties.[17]

The disadvantages of natural polymers are eliminated or reduced in synthetic polymers, where chemical and mechanical properties can be finely tuned.[17] Already FDA approved for use in degradable sutures and internal orthopedic fixations, polymers such as poly(lactic acid) (PLA), poly(glycolic acid) (PGA), and their copolymer PLGA, have been widely used in tissue engineering constructs.[16,17] These biocompatible polymers contain hydrolytic ester bonds that can be cleaved by the body's aqueous environment over time, where the byproducts can easily be metabolized to carbon dioxide and water within the body.[17]

Scaffold fabrication can be performed in numerous fashions, resulting in an array of geometries and architectures that can be tuned to meet nearly any desire. Mechanical strength, porosity, surface area, surface chemistry, unique geometry, and more must all be considered when designing a scaffold.[16] Scaffold architectures often represent meshes, sponges, fibers, and foams. These porous three-dimensional architectures have been shown to be desirable in tissue engineering applications to allow enhance nutrient diffusion, even cell distribution, and organized cell growth and differentiation.[14,16] To create these architectures, several fabrication techniques have been used, such as casting and leaching, gas foaming, emulsion freezing, electrospinning, rapid prototyping, and thermally induced phase separation.[14]

1.4 Electrospinning and Nanofiber Surfaces

Nanofiber fabrication by electrospinning is a popular and inexpensive way to produce polymeric fibers ranging from several nanometers to hundreds of microns of various composition.[16,18] An electrohydrodynamic process in which a potential differential is created between a polymer-solvent droplet and a targeted collector, electrospinning can create fibrous matrix that mimics that of the natural ECM.[18,19] The architecture of the matrix can be controlled by several features of the process, including polymer-solvent concentration, type of polymer and solvent, droplet to collector distance, electric potential magnitude, and droplet size.[19]

A relatively simple process, electrospinning requires three main components; a high voltage power supply, a capillary tube with a polymer solution, and a metal collecting plate.[20] The power supply creates an electric field between the capillary tube and the collector plate, charging the liquid particles in the polymer solution.[18–20] When the electrostatic forces between the polymer-solvent molecules overcome the surface tension of the solution at the capillary tip, a Taylor cone and polymer jet are formed.[18–20] As the polymer solution jet moves through the air towards the collector plate, the solution evaporates and only a string of polymer is left behind.[20] Using different shapes and movements of collectors, random or aligned fiber can be collected.[18,21] Coating polymer fibers in organic or biologically active molecules has also been shown to promote cellular functions.[21]

Mesenchymal stem cells (MSCs), bone cell precursors, are vital for the repair and maintenance of bone and connective tissue.[22] Synthetic nanofiber scaffolds have been shown to aid MSCs in differentiation, migration, and collagen production.[22,23] Initial MSC attachment and colony formation on fiber surfaces is increased compared to controls, an important factor during stem cell stability and differentiation.[24] Morphologically, SEM and immunofluorescent imaging

show that MSCs preferentially adhere, spread, and aggregate on nanofiber constructs.[24] Alkaline phosphatase, an important marker on bone differentiation and formation, is increased at three weeks compared to controls when MSCs are seeded on nanofiber scaffolds.[24] These important markers show that nanofiber scaffolds are a viable option in bone tissue engineering, but the exact intracellular mechanisms that cause cells grown on nanofibers to display these changes is not well understood.

1.5 Extracellular Sensing

The extracellular matrices of the musculoskeletal system are built to withstand the constant, repetitive compressive and tensile loading.[25] These structures shield the cells within from harmful forces, often only straining a few percent.[25] But, the small forces do act on musculoskeletal cells are vital in healthy bone formation and regulation.[26] Bone mass, for example, is continually adapted to meet the needs of the environment, remodeling in areas of constant wear and trauma.[26] To accomplish this remodeling, cells must be able to perceive the surrounding stresses and react to begin bone formation and remodeling. Osteocytes are the cells responsible for the conversion of mechanical loading to a signaling pathway, often called mechanotransduction.[26,27]

Mechanotransduction can be divided into three steps, mechanosensing, signal transduction, and effector-cell response.[28] Mechanosensing, the coupling of a mechanical force to create a biochemical response, is accomplished by a wide variety of cellular molecules, such as integrins, calcium channels, cadherins, and cytoskeletal components.[28] Once the proper mechanosensors are stimulated, intracellular enzymes like MAPKs, Cox-2, TNF-α, and Wnt/β-

catenin are activated. The initiation of these pathways results in the activation of a transcriptional factor, leading to gene expression and possible differentiation.[28]

The Wnt signaling pathway, for example, is a known factor for mechanotransduction in osteocytes, since mutations in this pathway has been shown to result in abnormal bone mass.[27] Wnt proteins, 19 different post-translationally modified glycoproteins, have four different signaling pathways; Wnt/β-catenin, planar cell polarity (PCP), Wnt/Ca^{+2}, and Protein Kinase A.[27] The most commonly studied pathway, Wnt/β-catenin, begins by the binding of a Wnt protein to a co-receptor complex.[27] By a downstream phosphorylation chain, this results on the inhibition of GSK-3β, which is responsible for phosphorylation β-catenin for degradation.[27] Without GSK-3β available β-catenin can permeate the cytoplasm, into the nucleus and affect gene transcription.[27] A prominent transcriptional factor, Runx2, is one of the many factors responsible for the differentiation of osteoblasts.[29]

Various other signaling pathways exist in mechanotransduction, many of which interact with each other. Papachroni *et. al.* summarized these interactions:

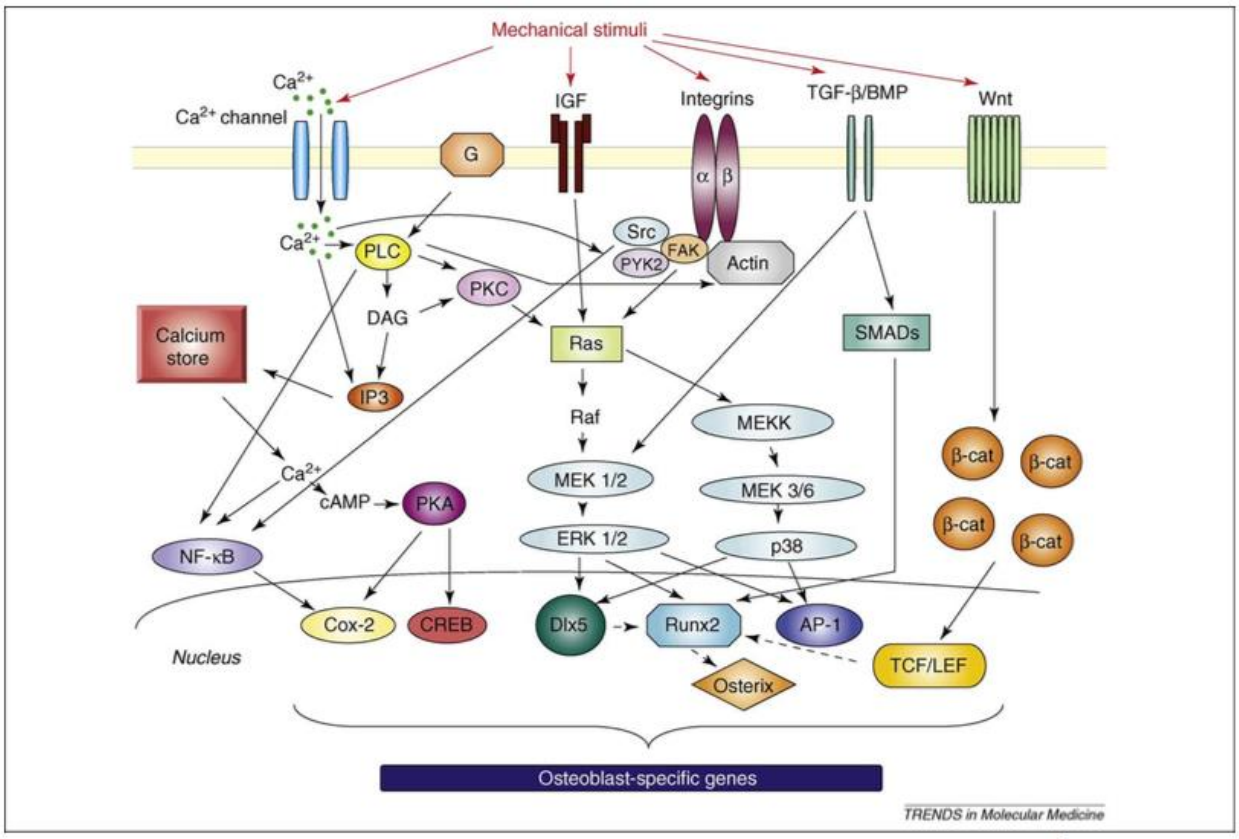

Figure 1. Schematic diagram of interactions of different signaling pathways during mechanical stretching

This diagram shows the complexity of the osteoblast mechanotransduction system. A complete understanding of these pathways will require further work in this area. One area of mechanotransduction to consider is ion signaling. Osteoblasts display an array of ion channel for calcium, sodium, and potassium to respond to mechanical, chemical, and electrical signals.[26] By manipulating the architecture of the synthetic ECM, research aims to more accurately control these cellular characteristics and others, without the need for soluble factors.

1.6 Mechanically Gated Ion Channels and Hypothesis

Bone cells contain several types of mechanosensitive, or mechanically gated, ion channels that will respond to membrane tension.[30] These channels are opened by forces in the plane of the membrane that cause the membrane to deform and stretch.[31] This stretching force is transmitted to the channel, causing it to open.[31] TREK-1, a member of the 2P-domain K^+ channel family, has been shown to be present in bone cells.[26] This trans-membrane ion channel functions as a non-inactivating voltage independent K^+ leak channel.[26] The channel has numerous possible functions such as maintaining resting voltage potential, cell volume control, and stable osmolarity.[26] It can also be activated by mechanical stimuli, such as membrane stretch and fluid flow.[26,31]

A study of how changes in an extracellular architecture affect the expression of TREK-1 has yet to be performed. Changes in the geometry and architecture have been shown to create stresses in the cellular membrane.[32] These stresses may cause changes in the function and expression of the TREK-1 channel. To better understand how this channel is expressed and operates is of significant value, since ion concentration is involved in MSC differentiation.[28]

We hypothesize that the expression of TREK-1 and other 2P-domain K^+ channels in preosteoblasts and MSCs can be influenced through alteration of a synthetic nanofiber extracellular geometry. Extracellular matrices, such as synthetic nanofibers, have been shown to cause stem cells and precursor cells to begin differentiation. These ECMs have also been shown to increase membrane stretching, one of the stimuli that can cause the channels to open. By seeding cells on various synthetic nanofiber architectures, then analyzing their growth and protein expression, we will look to shed light on how the expression of TREK-1 changes in response to these variations.

Chapter 2

Methods

2.1 Slide Preparation

PVA Cover Slip Synthesis

Experimental glass covers lips were first coated in poly(vinyl alcohol) (PVA) to prevent cell adhesion to the slides surface and promote focal adhesion contact to nanofibers. Glass covers lips (22mm x 22mm) were washed on an orbital shaker at 60 rpm in a bath of isopropyl alcohol and potassium hydroxide for 30 minutes. The cover slips were then removed from the bath and rinsed overnight in distilled water. A bath of 1% 3-(amino)propyl-trimethoxysilane (Sigma-Aldrich) in acetone was used to silanize the cover slips for 10 minutes on an orbital shaker at 60 rpm. Cover slips were rinsed with distilled water for 5 minutes twice, before being blown dry with nitrogen gas and cured on a hot plate at 65^{o}C for 2 hours. A bath of 0.5% glutaraldehyde in distilled water was used to activate the slides by washing them in this solution for 30 minutes. The cover slips were then washed in distilled water for 10 minutes twice and once in distilled water for 30 minutes. All surfaces were blown dry with nitrogen gas and stored at 4^{o}C overnight until the next step.

A 5.6% PVA stock solution was made by diluting PVA (molecular weight ~98,000; 98% hydrolyzed; Sigma-Aldrich) in distilled water. The mixture was solubilized in a ~90^{o}C water bath, then immediately 0.2 μm filtered to remove impurities. To create the coating solution, 1124 μL of 2 N HCl was added to 8876 μL of the filtered PVA solution. Activated glass cover slips, from the previous procedure, were covered in 100μL of this solution, and then incubated for 3 minutes. After incubation, a pipette tip was used to re-spread the solution over the slips so the

entire surface was covered. The cover slips were immediately spun for 40 seconds at an acceleration of 550 rpm to a maximum speed of 7000 rpm using a spincoater (Laurel Technologies). After spinning, PVA cover slips were cured overnight at 4^{o}C.

PMMA Cover Slip Synthesis

Control glass cover slips were made to compare cell growth and expression to the experimental group. These cover slips were coated in the same polymer later used to make nanofibers. First, the glass cover slips were cleaned with acetone and blown dry to remove any impurities. A 5% PMMA solution was made by dissolving PMMA (molecular weight ~996,000; Sigma-Aldrich) in nitromethane. Cover slips were coated in 100 μL of this solution and immediately spun for 40 seconds at an acceleration of 550 rpm with a maximum speed of 7000 rpm. Occasionally cover slips would not spin flat, resulting in a misshapen film. This can be corrected by adding a drop of nitromethane to the cover slip and respinning. Coated covers lips were allowed to dry overnight at room temperature before use. Additional cover slips were stored at room temperature.

2.2 Nanofiber Synthesis

Synthetic nanofibers of PMMA were synthesized using electrospinning onto PVA coated glass cover slips. The electrospinning apparatus consisted of a clear acrylic walls, metal stand with a syringe pump (New Era Pump Systems, Inc.), a high voltage source, and a plain copper target 15 cm x 15 cm. A 4.4% PMMA solution was formed by dissolving PMMA (molecular weight ~996,000; Sigma-Aldrich) in 60:40 (vol/vol) of N, N-dimethylformamide and tetrahydrofuran. This solution was loaded into a 10 mL syringe (BD Syringes) with a 30 gauge 1

inch blunt tip needle (SAI Infusion Technologies). A metal wire was attached from the needle to the voltage source and out to the copper collecting plate target, as seen in Figure 2. Generic scotch tape was used to secure a PVA coated slip to the copper plate target. A distance of 15 cm was set from the tip of the needle to the cover slip. A potential differential of 15 kV was applied with a pumping rate of 0.6 mL/hr for 2 minutes. Ambient conditions inside the electrospinning box included a temperature from 20-25ºC, humidity 30-60%, and atmospheric pressure 747-753 mmHg.

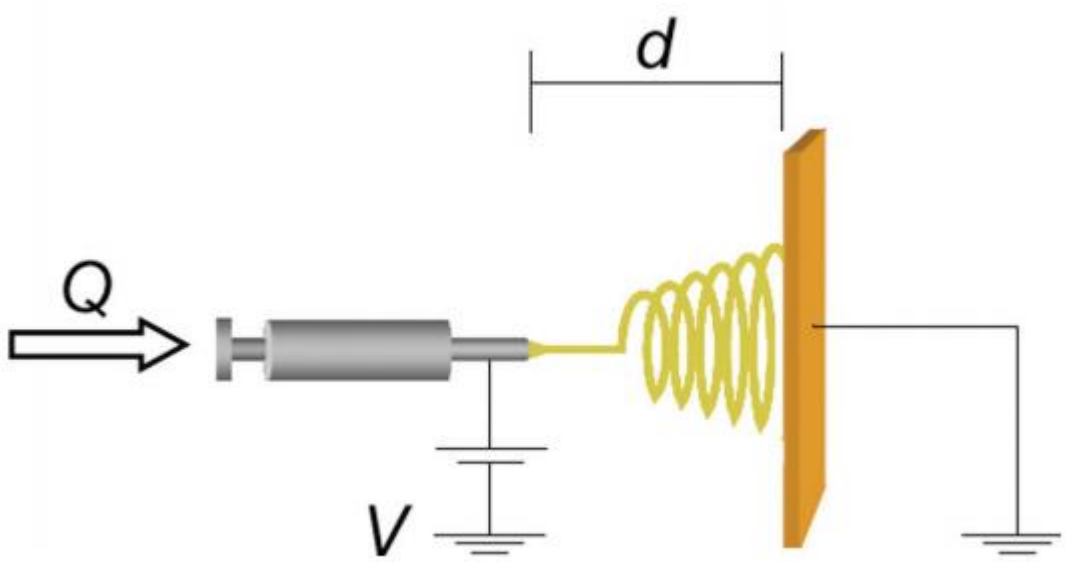

Figure 2. Typical electrospinning setup. Q, flow rate; d, distance between plate and needle; V, applied voltage.[18]

Once the fibers were spun onto the cover slips, fiber quality was visually inspected under bright field microscopy to ensure relatively consistent fiber density and architecture. Cover slips and fibers were then heated for 5 minutes to 105ºC, the glass transition temperature of PMMA, for better adhesion to the glass surface. As seen in Figure 3, thin line of

Norland Optical Adhesive 68 was placed on each edge of the cover slips and hardened under UV light, to ensure fiber stability during cell culture in media. Once the glue had set, prepared slides were stored at room temperature until needed.

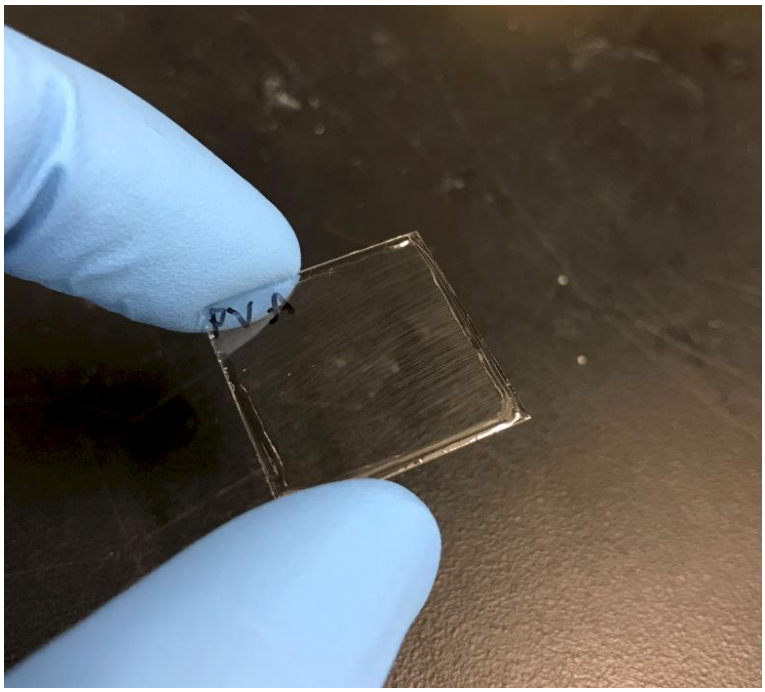

Figure 3. Glass cover slip with electro spun PMMA fibers. UV set glue has been used to hold down fiber edges during cell culture.

2.3 Cell Culture

Cell Thawing

All open cell culture procedures were performed in a cell culture hood (Nuaire Labgard ES Class II Type A2 Biological Safety Cabinet). MC3T3 a mouse osteoblast precursor, MG63 human osteosarcoma, and human mesenchymal stem cell lines were obtained from GIBCO and stored at -80^{o}C in 1.0 mL vials. To culture these cells, the vials were thawed in a 36^{o}C water bath and immediately emptied into a 15 mL centrifuge vial. At least twice the amount of alpha-modified minimum essential medium (α-MEM) (GIBCO), with 10% (vol/vol) fetal bovine

serum (FBS) (Atlanta Biologicals and 1% (vol/vol) penicillin/streptomycin (Pen/Strep) (Lonza), was slowly added to the existing solution, then centrifuged for 5 minutes at 300g (Thermo Scientific Heraeus Multifuge X1). Following centrifuging, the supernatant was aspirated and the cells were resuspended in media. To obtain the required cell counts for seeding, cells were cultured in 15 cm diameter cell culture dishes (Greiner Bio-one Cellstar) in a humidified incubator (Nuaire Autoflow IR Direct Heat CO_2 incubator) until the necessary confluency was reached.

Cell Feeding and Passage

The cell media was aspirated and new media (α-MEM) with 10% FBS and 1% Pen/Strep was used to replace it every 48-72 hours. Cell passage was carried out when confluency reached 70-90%. The media was aspirated and the cell dish was washed briefly in Phosphate Buffer Solution (PBS), which was prepared with concentrations of 0.135 M NaCl (Sigma-Aldrich), 2.7 mM KCl (Sigma-Aldrich), 1.6 mM $Na_2HPO_4 \bullet 7H_2O$ (Sigma-Aldrich), and 1.8 mM KH_2PO_4 (Sigma-Aldrich) in deionized and distilled water, adjusted to a pH of 7.4 using NaOH (Sigma Aldrich) and HCl (Sigma-Aldrich), and filtered using bottle top filtration (VWR). The PBS was then aspirated and a quarter of the original media volume of Trypsin-EDTA (Mediatech, Inc.) was added to the dish. Cells were incubated in the Trypsin-EDTA for 5 minutes to allow the cells to detach, as verified under bright field microscopy. Occasionally, gently tapping the side of the cell culture dish against a hard surface, such as the side of a desk, was necessary to detach all cells. A portion of the Trypsin/cell suspension was centrifuged for 5 minutes at 300g. The supernatant was aspirated and the pellet was resuspended in new media (α-MEM) with 10% FBS and 1% Pen/Strep, then added to a new dish.

2.4 Scaffold Seeding

Under a cell culture hood, each prepared coverslip was placed polymer side up into the well of a 6 well cell culture dish (Greiner Bio-one Cellstar). All 6 well cell culture dishes were then left open and sterilized by UV light for 20 minutes. Once sterile, the cell culture dishes were closed while the cells were prepared for seeding. Media was aspirated from the 15 cm diameter cell culture dish and the dish was washed with 1X PBS. A quarter of the original media volume of Trypsin was added and the cells were allowed to incubate for 5 minutes. If detachment was not seen under bright field microscopy after 5 minutes, the side of the cell culture dish was tapped to aid in detachment. Once all cells were detached, the Trypsin/cell suspension was centrifuged for 5 minutes at 300g. The supernatant was aspirated and smaller amount of new media (α-MEM) with 10% FBS and 1% Pen/Strep was used to resuspended the pellet. A hemocytometer was used to calculate the cell density in 0.1 mm^3 of the resuspended solution. This value was used to calculate how much volume of the suspension was needed to obtain the 10,000-20,000 cells/cm^2 (varied depending on which test was being run) in the required number of 6 well plates. Once that density was reached, the final suspension was distributed amongst the 6 well plates, 2 mL per well, taking care to ensure the cover slips did not float on top of the media.

2.5 Immunofluorescence Imaging

To view proteins and structures of interest, cover slips were imaged using immunofluorescence imaging after a set period of growth. Cytoskeletal Stabilization Buffer (CSB) was prepared in distilled water with 50 mM NaCl (Sigma-Aldrich), 0.5% Triton X100, 10

mM PIPES (Sigma-Aldrich), 2.5 mM $MgCl_2$ (Sigma-Aldrich), 1 mM EGTA (Sigma-Aldrich), 0.3 M Sucrose (Sigma-Aldrich), protease and phosphatase inhibitors (100 μL per 10 mL for each, Thermo Scientific), and adjusted to a pH of 6.8 using NaOH (Sigma Aldrich) and HCl (Sigma-Aldrich). Fixation Buffer (FB) was prepared in 1X PBS with 3.7-4% paraformaldehyde (Sigma Aldrich). Permeabilization Buffer (PB) was prepared in 1X PBS with 3% Bovine Serum Albumin and 0.1% Triton X100.

For the following section a 'wash' will be defined as allowing the solution to sit in the well, no shakers or orbiters. Cover slips were first briefly washed in 1mL of 1X PBS, and then aspirated. Next cover slips were washed in 500 μL CSB for 1 minute, and then aspirated. Cover slips were incubated in 500 μL of FB for 15 minutes, aspirated, and washed again in 1X PBS, then aspirated. Next, cover slips were incubated for 45 minutes in 500 μL PB, then aspirated. The primary antibody (Vinculin or TREK-1; Santa Cruz Biotechnologies, Inc.) of interest was added (1:500 in PB) and incubated for 1 hour at room temperature, the aspirated. Cover slips were then washed for 5 minutes in PBS 3 times. The secondary antibody (680 rabbit anti-mouse and 488 mouse anti rabbit; Rockland) of interest was added (1:500 in PB) and incubated for 45 minutes in the dark at room temperature, then aspirated. Cover slips were again washed for 5 minutes in PBS 3 times. Phalloidin (Biotium) at 1:1000 in PB and DAPI (VWR) at 1:5000 in PB were added and incubated in the dark at room temperature for 30 minutes. Cover slips were again washed for 5 minutes in PBS 3 times.

Cover slips were then mounted onto glass slides (VWR) using ~50 μL of Fluoro-Gel, (with Tris Buffer) (Electron Microscopy Sciences). Generic clear nail polish was used to seal the coverslips by painting the 4 edges to the glass slide. A Leica DM 5500B microscope was used to image the slides. The following objectives were utilized during imaging; air 20x/0.35 (506248),

water 10x/0.30 (506142), and water 40x/0.80 (506155). A Leica DFC360 FX camera was used to capture the images and Leica LAS software was used to control the microscope.

2.6 Western Blotting

SDS-PAGE Gel Preparation

All western blot equipment (Hoefer, Mighty Small II for 8x9cm Gels) that came in contact with the gels was clean in soap/water, ethanol, and distilled water. The gel casting equipment was prepared and tested for leaks using distilled water. In order to run two gels simultaneously, 20 mL of 10% SDS-PAGE running gel was made using 9.592 mL distilled water, 5 mL 40% acryl-bisacrylamide (Amresco), 5 mL 1.5 M Tris (pH 8.8), 0.2 mL 10% SDS (Sigma-Aldrich), 0.2 mL 10% ammonium persulfate, and 0.008 mL TEMED. This solution was distributed to the two gel casters, adding the ammonium persulfate and TEMED just before distribution. Isopropyl alcohol was added to the top and the solution was allowed to harden for ~45 minutes until the gel was set. The stacking gel was prepared using 5.832 mL distilled water, 1 mL 40% acryl-bisacrylamide (Amresco), 1mL 1.5 M Tris (pH 6.8), 0.08 mL 10% SDS (Sigma-Aldrich), 0.08 mL 10% ammonium persulfate, and 0.008 mL TEMED. The final two components, ammonium persulfate and TEMED, were not added until just before the solution was distributed to the casting set-up. Once the stacking gel was added to the cast, a 12 well comb was fitted to the casting set-up and the stacking gel was allowed to harden in ~10 minutes. If the gels were stored overnight, a damp paper towel was placed over top of them to prevent drying.

Sample Preparation and Loading

Cover slip samples to be tested were lysed, with RIPA sample buffer with 10X-Triton and 1% (vol/vol) of Holt protease inhibitors, after cells had grown for the desired time point. Lysates were then frozen for at least 48 hours before beginning the Western Blot procedure. To begin the procedure, thawed samples were added in a 6:1 ratio with laemelli and vortexed to mix thoroughly. Samples were then boiled at 95^{o}C for 10 minutes before centrifuging briefly.

Prepared samples were then loaded into the gel with a molecular ladder on either side. Empty lanes were filled with blank lysis buffer and laemelli at a 6:1 ratio. The gels were then placed under a potential differential of 120 Volts for 3-4 hours in a running buffer at 4^{o}C consisting of 1.7% (wt/vol) Tris-Glycine Buffer and 2% (vol/vol) of 10% SDS in distilled water. The progress of the gels was monitored by the molecular ladder.

Transfer

A transfer solution was prepared that consisted of 1.7% (wt/vol) Tris-Glycine Buffer and 20% methanol in distilled water. The gels were removed from the casting plates and placed onto of an methanol activated polyvinylidene fluoride (PVDF) membrane (Licor). These were set between a series of filter papers and sponges for protection. This membrane/gel sandwich was placed in the transfer buffer at 4^{o}C and a potential differential of 80 volts was applied for 80 minutes. After the transfer was complete, the membranes were blocked with 5% bovine serum albumin (BSA) (VWR) in TBST for an hour at room temperature or overnight at 4^{o}C.

Immunostaining and Imaging

The blocking solution was removed and the primary antibody (α-tubulin at 1:400 and TREK-1 at 1:100; Santa Cruz Biotechnologies, Inc.) was added in TBST and 5% BSA. This was

slowly rocked for 1 hour at room temperature or overnight at 4^{o}C, and then removed. After the primary solution was removed, the membranes were washed for 5 minutes in TBST 3 times. The secondary antibodies (680 mouse anti-rabbit at 1:1000 and 800 rabbit anti-mouse at 1:1000; Licor) were added in TBST and 5% BSA. This solution was rocked for 1 hour at room temperature, and then removed. The membranes were again washed for 5 minutes in TBST 3 times.

Membranes were imaged using a Licor Odyssey Scanner. The channel intensity was adjusted to eliminate saturation. The Licor Odyssey software was used to identify protein bands and quantify the signal intensity for each band. The values were exported to excel for further analysis. Protein of interest bands can be normalized to 'house-keeping' proteins to quantify relative changes in protein expression

2.7 ELISA and PicoGreen Assay

A TREK-1 ELISA kit (MyBioSource Inc.) was used on a variety of samples. First 50 uL of standard, sample, or sample diluent was added to each well in duplicates. Next 50 uL of HRP (horse-radish peroxidase) was added to each well and the assay was incubated at 37 degrees Celsius for 60 minutes. Each well was then emptied and washed four times with 300uL of 1x washing solution. Next, chromogen A and B where added to each well, successively and incubated for 15 minutes at 37 degrees Celsius. The stop solution was added after incubation and the assay was imaged for absorbance at 450nm using a fluorescence microplate reader (TECAN Infinite 200PRO).

A Picogreen assay (ThermoFisherSci, Inc.) was used to analyze the same samples as the TREK-1 ELISA. To perform the test, a 96-well plate (Greiner Bio-one Cellstar) was used. First a high standard curve was created by serial dilution from 200 ug/mL dsDNA in TE buffer; 1 ng/mL – 1 ug/mL, with 50 uL/well. Next, a low standard curve was created from the same stock dsDNA solution; 25 pg/mL – 25 ng/mL, also with 50 uL/well. The samples were diluted to 20% in TE buffer to a volume of 50 uL in each well, with all samples duplicated. Next, 50 uL of Quant-iT PicoGreen reagent, diluted 200-fold from the stock solution, was added to each well including the standard curve wells. The assay was allowed to incubate 5 minutes prior to imaging using a fluorescence microplate reader (TECAN Infinite 200PRO) with an excitation of 480nm and an emission of 520nm.

Chapter 3

Results

3.1 Nanofiber Synthesis

Several qualitative trends were observed during the electrospinning process. Varying the geometry of the copper background plate gave rise to changes in general shape of nanofiber deposition. A large plain plate with a cover slip in the center led to randomly oriented fibers with a mix of straight and curled fibers. If insulation was added to the copper plate to cover all but two exposed areas on each side of the coverslip, unidirectional fibers were formed. Other variations in electrospinning parameter resulted in changes in the diameter of the nanofibers. A more dilute polymer solution formed fibers with a narrower diameter, while a solution that is too dilute resulted only in spattering, the deposition of non-continuous droplets on the coverslip. Increasing the distance from the tip of the needle to the collection plate had a similar effect; the shorter the distance, the larger the fiber diameter.

It was attempted to maintain an even distribution of fibers on the PVA surface, but variation in the deposition of electrospinning was observed. We speculated that this was a result of the electrostatic forces from the tape used to hold the glass coverslip to the background. At times a pattern could be observed that closely resembled the shape of the tape underneath. In order to combat the problem, steps were taken to limit the levels of static electricity on the tape. One of the most effective methods was to use tape that had been pulled from the reel several hours prior to use. This may have allowed the static electricity to dissipate from the tape. Other methods included increasing the humidity during electrospinning and rolling the tape across a piece of fabric.

3.2 Immunofluorescence Imaging

Images of MC3T3 cells grown on PMMA nanofibers are shown below in Figure 4. Cells appear to form focal adhesions on the nanofibers, as evidenced by the presence and placement of vinculin, labeled in green. Images of MG63 cells grown for 3 days on flat PMMA control surfaces are presented below in Figure 5. TREK-1, labeled in green, is present in a majority of cells. It is distributed throughout the body of the cell, located on the cell membrane. Images of MG63 cells grown for 3 days on PMMA fibers are displayed in Figure 6. The images also show the presence of TREK-1, labeled in green. The transmembrane protein is dispersed throughout the body of each cell, with less visible protein concentration near the apparent focal adhesions. These images show that the cells adhere to the PMMA nanofibers and express the TREK-1 protein, both on flat and nanofiber surfaces.

In Figure 4 several prominent focal adhesions are indicated using arrows. Notice that these focal adhesions lie along the nanofibers, indicating that the cells are attached to the nanofiber matrix. As seen in Figure 6-C, TREK-1 tends to be distributed through the body of the cell, instead of the lamellipodia. This can be expected since TREK-1 is a potassium leak channel used to maintain a specific cell potential and greater expression around the cell body would be more useful than near the edges of the cell.

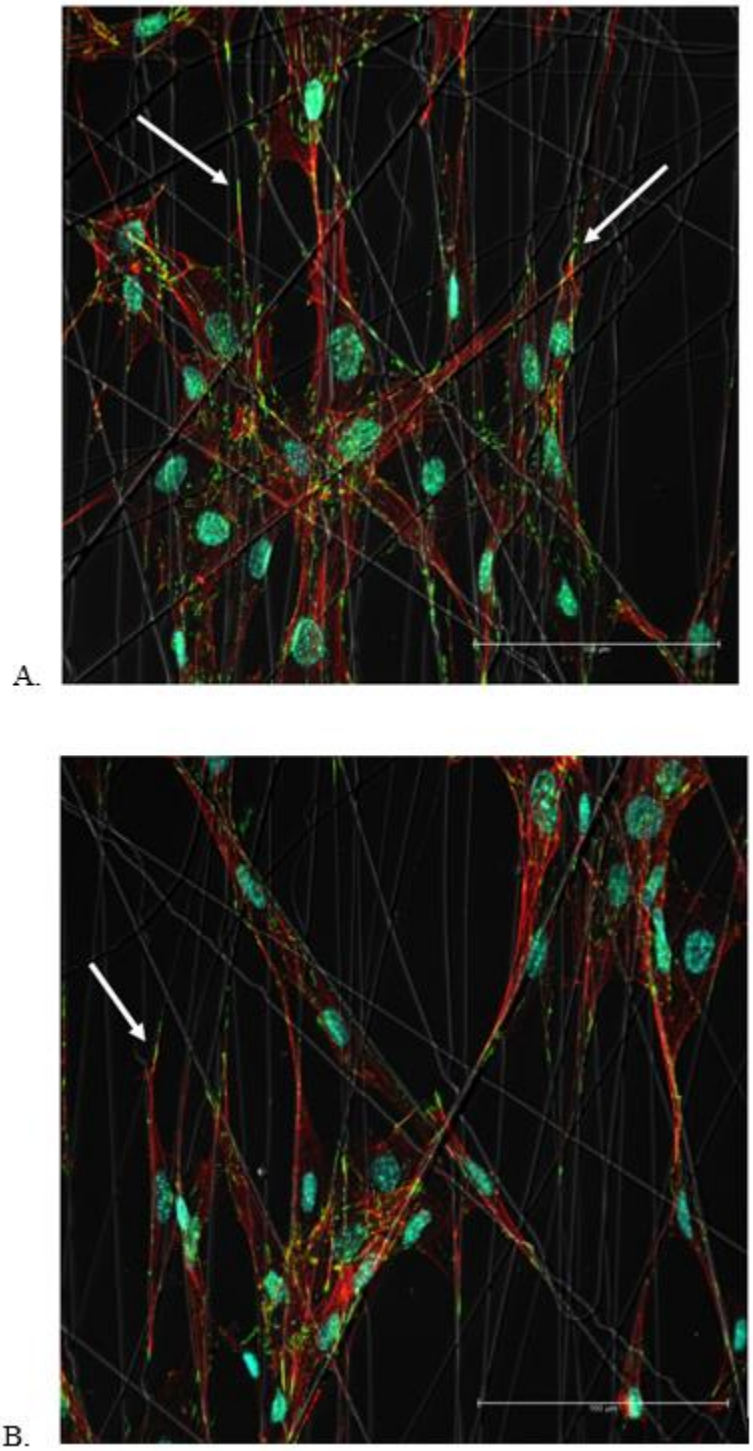

Figure 4. MC3T3 cells cultured on PMMA nanofibers for 72 hours. Cell nuclei are labeled in blue while the actin cytoskeleton, labeled in red, shows how the cells stretch along and conform to the fiber architecture. Labeled in green, vinculin and focal adhesions are localized to the outer edges of the cell.

A.

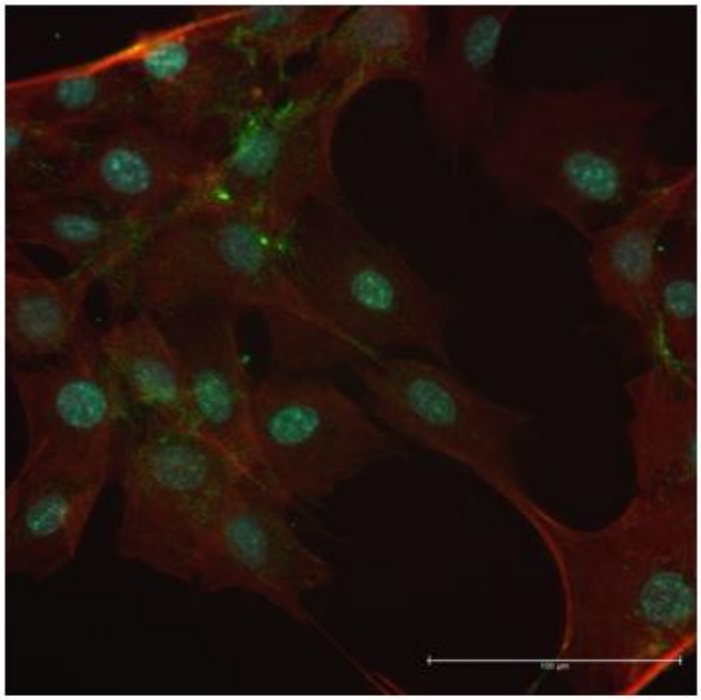

B.

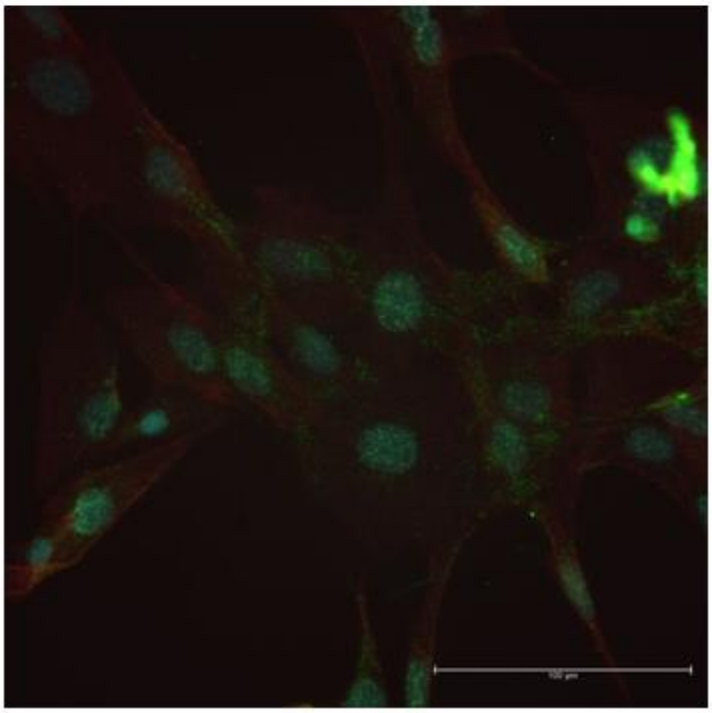

Figure 5. MG63 cells cultured on flat PMMA surfaces. TREK-1 is labeled in green and is expressed over the body of the cell. It should be noted that in B, the large bright green spot is likely to be an imperfection in imaging.

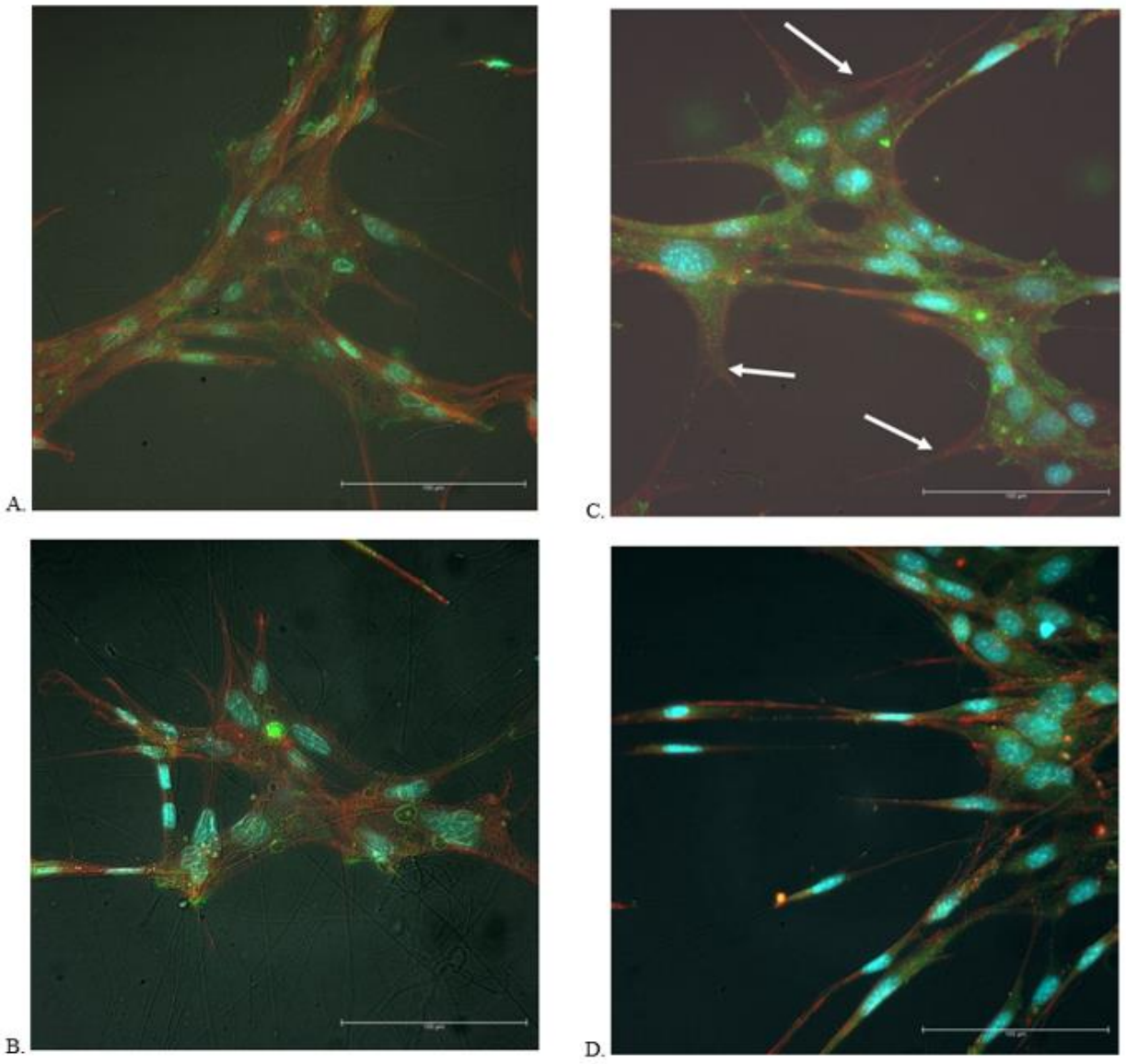

Figure 6. MG63 cells cultured on PMMA nanofibers for 3 days. TREK-1 is labeled in green and can be seen distributed throughout the cell body of most cells.

3.3 Western Blotting

The purpose of this study was to investigate the effects of extracellular nanofiber architecture on TREK-1 expression. Overall, western blot results show consistent levels of TREK-1 present in cells on flat surfaces. On the other hand, cells on fiber surfaces displayed varying levels of TREK-1 as measured by western blotting. The housekeeping protein, α-tubulin was used to normalize to the relative number of cells. The results of a western blot on three slides with nanofibers and three slides with flat polymer cultured with MC3T3 cells can be seen below in Figure 4-4. As shown by the error bars, which display standard deviation, levels of TREK-1 are more consistent on flat surfaces. On the other hand, the variation of TREK-1 on nanofiber surfaces resulted in a larger standard deviation. Figure 4-5 displays the bands that this data was derived from. Figures 4-6,7 are also western blot results from separate MC3T3 cultures and display similar trends.

Western blotting performed on MG63 cells showed mixed results. One analysis revealed similar levels of TREK-1 on both nanofiber and flat surfaces, while another showed a difference between the two groups. The resulting average normalized intensities can be seen below in Figure 4-8 and the western blot images can be seen in Figure 4-9.Results from four separate western blots of hMSCs cultured on nanofiber and control surfaces show results similar to those of the MG63 results. Several analyses show slight increases in TREK-1 expression on nanofiber surfaces over control surfaces, while others show no change. These results are displayed in Figure 4-10.

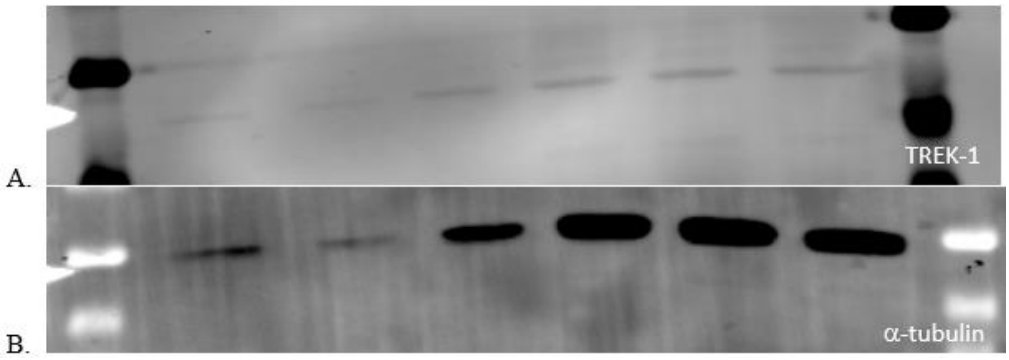

Figure 7. Western blot bands of MC3T3 cell lysates with A) TREK-1, the protein of interest, and B) α-tubulin to normalize. The first three bands represent cells grown on nanofiber surfaces while the second three bands represent cells grown on flat surfaces. Note that the TREK-1 bands are relatively similar, but since the α-tubulin bands of the flat surfaces are of greater intensity, the normalization results in increased TREK-1 per cell on the fiber grown samples.

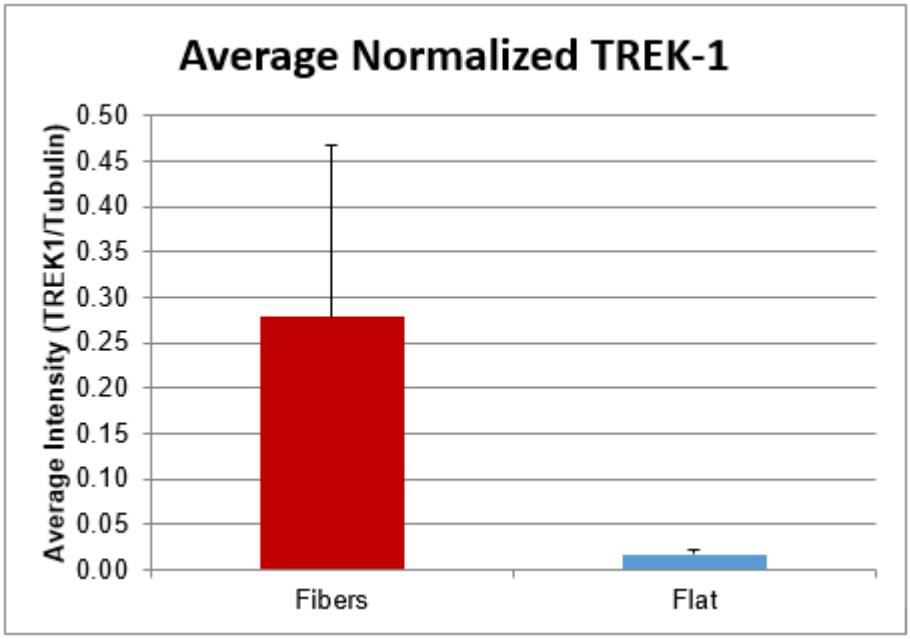

Figure 8. Western blot results of MC3T3 cells for TREK-1 normalized to α-tubulin on three nanofiber slides and three control slides. Note the lower standard deviation on the flat surfaces as indicated by the error bars.

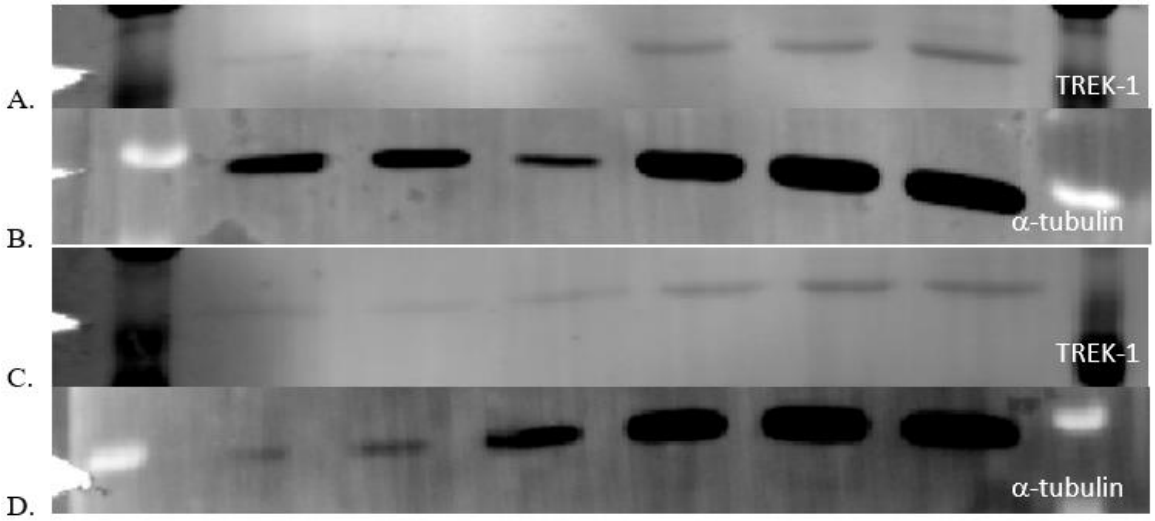

Figure 9. Additional western blot images from MC3T3 cell samples. The first three lanes are from cells cultured on nanofibers, the second three lanes are control samples grown on flat surfaces. Images A and B are from the same samples, while images C and D are from the same samples.

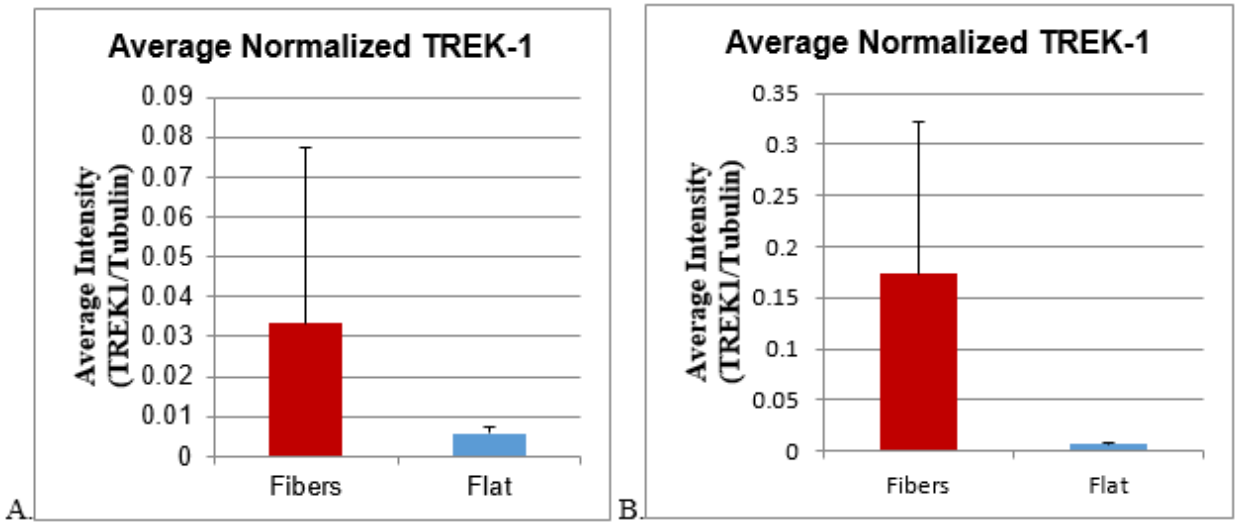

Figure 10. Additional western blot results from MC3T3 cell samples of TREK-1 normalized to α-tubulin. These results display similar trends compared to the initial results, as the standard deviation of the flat surfaces in lower than that of the nanofiber surfaces. Data for the graph A is from ima images A and B of Figure 9, while data for graph B is form images C and D of Figure 9.

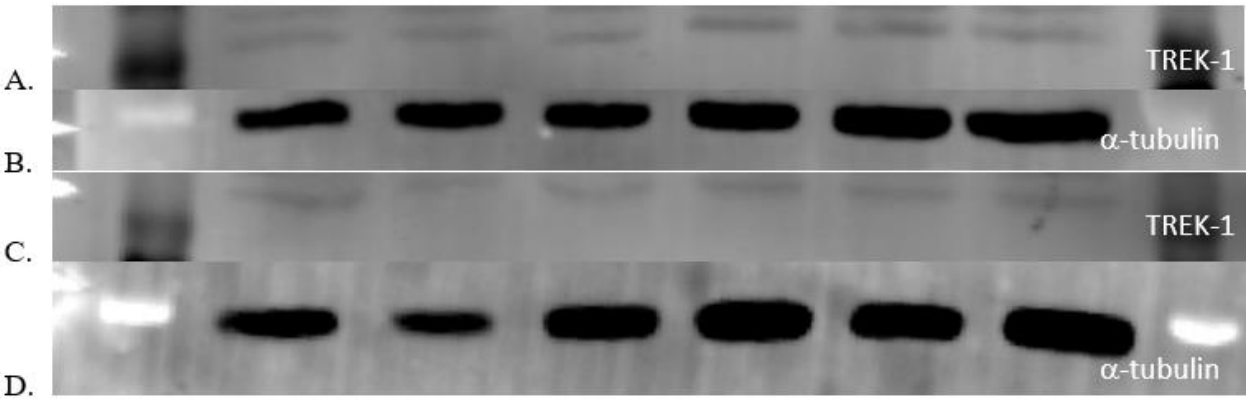

Figure 11. Western blot images from MG63 cells cultured on nanofiber and control surfaces. The first three lanes are from cells cultured on nanofibers, the second three lanes are control samples grown on flat surfaces. Images A and B are from the same samples, while images C and D are from the same samples.

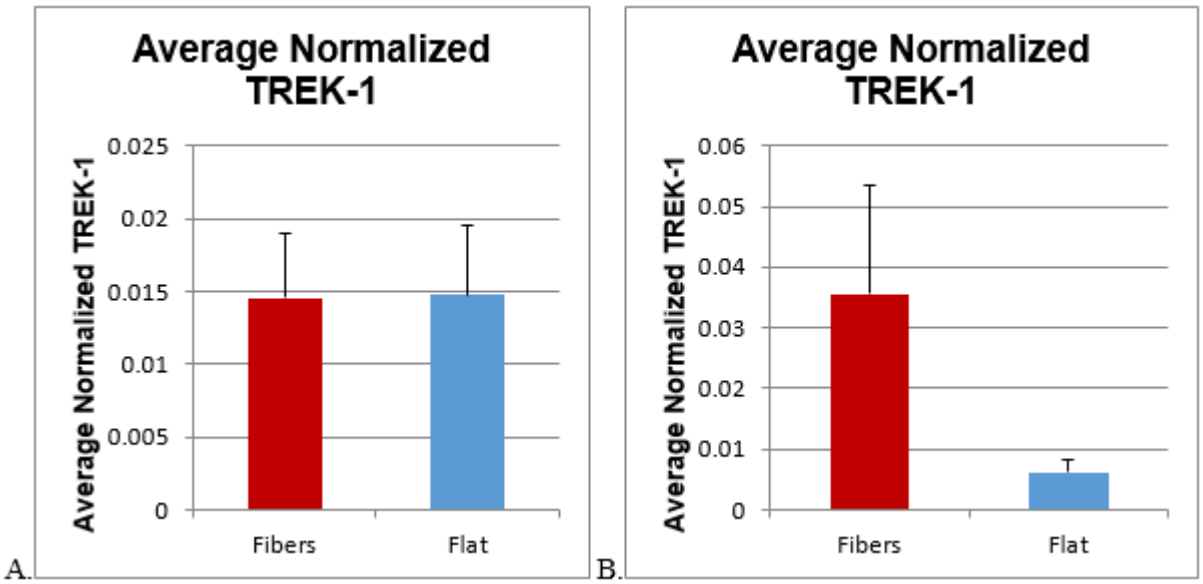

Figure 12. Western blot results from MG63 cells of TREK-1 normalized to α-tubulin cultured on nanofiber and control surfaces. Graph A shows no noticeable difference between the two group, while graph B shows results similar to the previous analysis with MC3T3 cells.

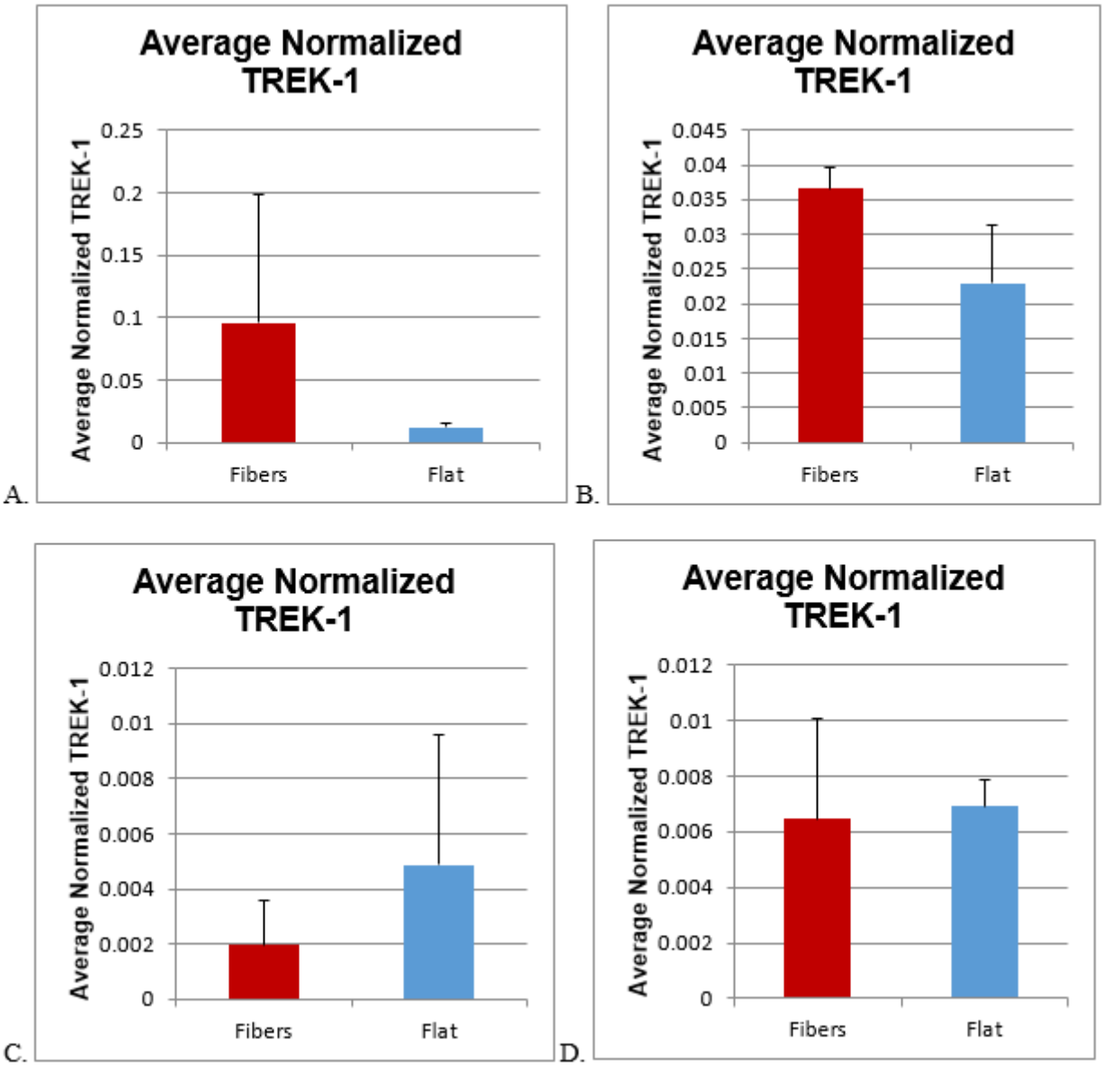

Figure 13. The results of four separate western blots of hMSCs for TREK-1 normalized to α-tubulin on 12 nanofiber slides and 12 control slides. Graphs A and B show increases in TREK-1 expression on nanofiber slides, while graph C displays a decrease and graph D display no change.

3.4 ELISA and PicoGreen Assay

Raw ELISA/PicoGreen data was collected from hMSC samples cultured on a variety of nanofiber sizes, in addition to several of the samples used to perform previous western blots. The PicoGreen assay, displayed below, shows low levels of emission of the 520nm wavelength. Figure 14, the results of a PicoGreen assay from a range of nanofiber diameters, shows a larger concentration of DNA of flat surfaces, therefore indicating a larger number of cells.

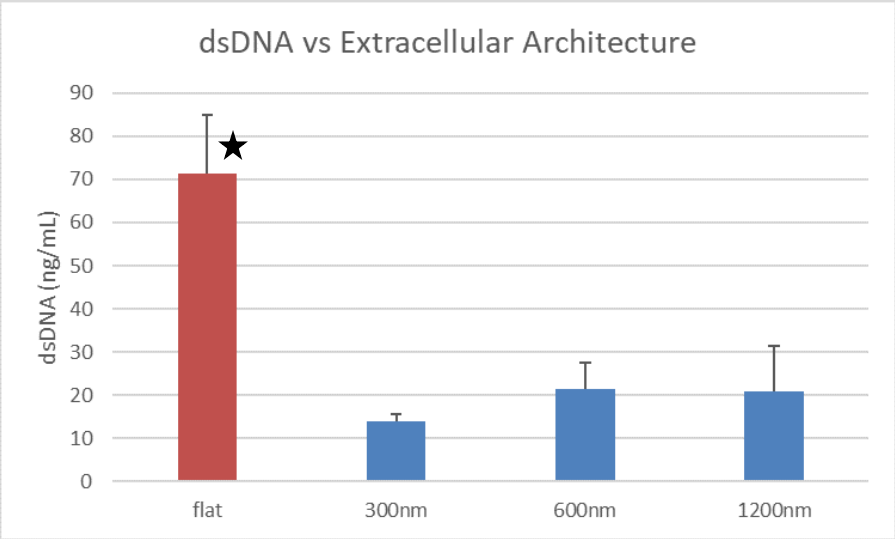

Figure 14. A PicoGreen assay of hMSCs on various fiber diameters and flat surfaces. Using a standard curve, the assay can determine dsDNA concentrations. (*p<0.05)

The results of the TREK-1 ELISA were inconclusive. The absorbance of the blank/control wells was higher than the absorbance of the sample wells. But, if the blank/control well values are not subtracted from the sample values, a trend can be observed. As seen in Figure 15, higher concentrations of TREK-1 were found in the 300 and 600 nm samples compared to the flat and 1200nm samples, although this data was not found to be significant due to low sample numbers.

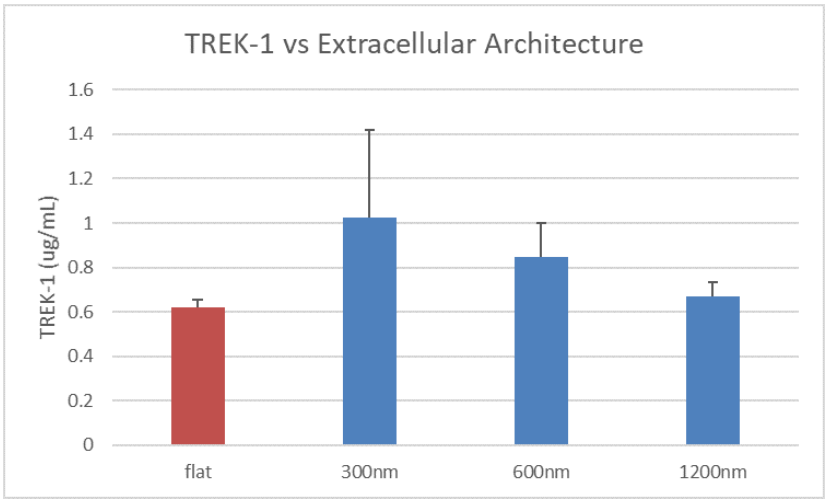

Figure 15. Unadjusted TREK-1 concentrations on various fiber diameters. No significance was found (p=0.19).

However, an assay on other samples used for western blotting revealed slightly significant data. Shown in Figure 16 below, flat surfaces had a lower expression of TREK-1 compared to fiber surfaces (300nm).

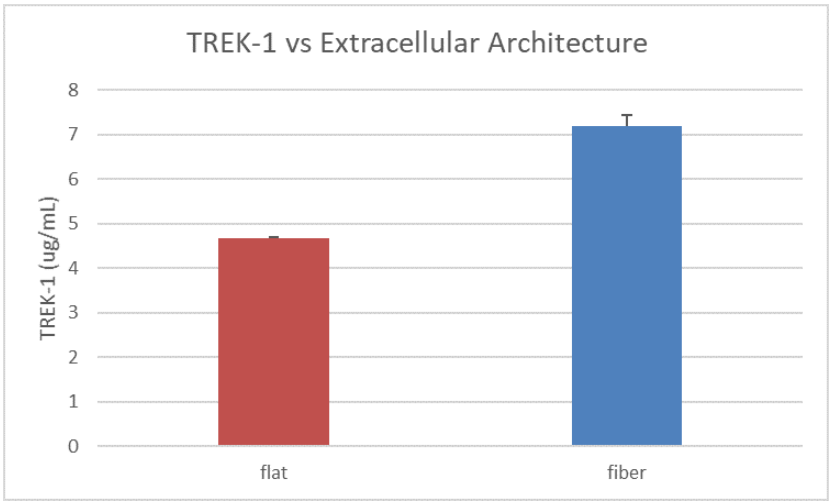

Figure 16. Unadjusted TREK-1 concentrations in hMSCs cultured on flat and nanofiber surfaces. Fiber surfaces show an increase in TREK-1 concentration. (p<0.05)

By normalizing TREK-1 concentrations to dsDNA concentrations, the relative amount of TREK-1 expressed per volume of lysate can be obtained. When this is performed on the data in Figure 16, it displays a statistically significant trend shown in Figure 17.

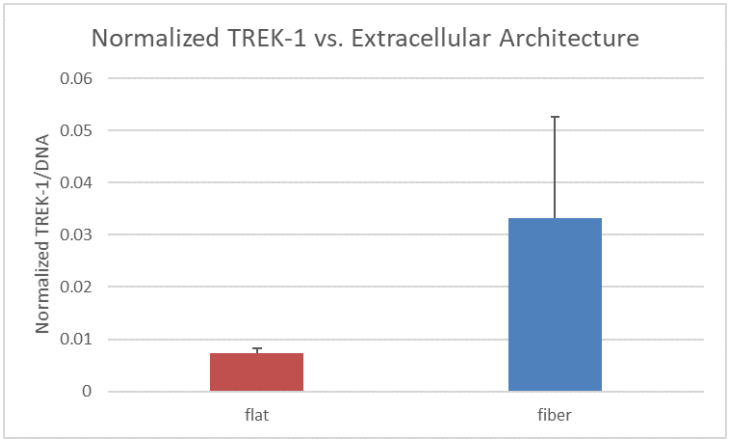

Figure 17. Normalized TREK-1 expression to dsDNA in hMSCs shows in increase in TREK-1 expression compared to on fiber surfaces. ($p<0.005$).

When TREK-1 expression was compared in other fiber diameters, a trend was observed, but a large standard deviation and no statistical significance was were found. This data can be observed in in Figure 18 below.

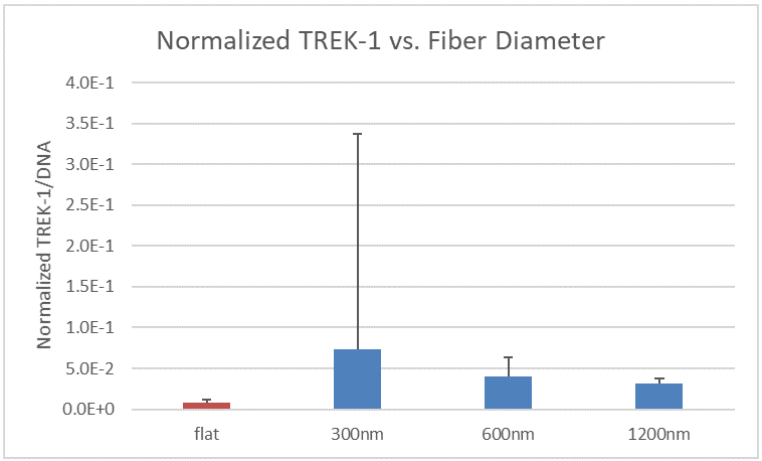

Figure 18. Normalized TREK-1 expression to dsDNA in hMSCs shows an insignificant increase in TREK-1 at low nanofiber diameters.

Chapter 4

Discussion

4.1 Nanofiber Synthesis

The synthesis of nanofiber resulted in mostly straight fibers, randomly oriented on the PVA surface. Nanofibers can be easily synthesized by a variety of techniques and have been used by several research areas and industries to construct various designs. Electrospun nanofibers are an excellent choice to model the extracellular matrix due to the control of their size and shape, the ease in cell binding, and the inexpensive use.

By modeling the extracellular matrix with nanofibers and altering various parameters, we can study the effect that the extracellular architecture has on a cell. This can be beneficial since altering an extracellular geometry to induce cell changes can often be less expensive and time consuming than harvesting and purifying the required protein or growth factor.

We were able to construct nanofibers of various diameter in order to study their effects on the expression of a transmembrane potassium channel, TREK-1. While the nanofibers synthesized for this investigation were able to show some trends, a larger array of shapes and sizes could be investigated to better understand how these fibers alter the gene expression of transmembrane potassium channels.

4.2 Immunofluorescence Imaging

Cell imaging allows for the verification of presence and a qualitative localization of the protein of interest. In Figure 5&6 it can be seen that TREK-1 is present in MG63 cells, but not

localized to a particular area of the cell, like vinculin in a focal adhesion as seen in Figure 4. It can be observed, however, that a majority of the TREK-1 is present in the body of the cell, as indicated in Figure 5&6 by apparent increases in TREK-1 intensity. This can be expected since most transmembrane proteins are concentrated to the body of the cell rather than the pseudopodia. Expression of TREK-1, and other ion channels, in the cell body are used to maintain the concentration of ions and intracellular voltage potential. Therefore, we would expect to observe this protein dispersed through the body of the cell.

4.3 Western Blotting

Western blots are primarily used to identify the presence of protein of interest and attempt to quantify the expression levels of that protein. Through the use of a primary and secondary antibody, the protein is fluorescently labeled and can be viewed using a fluorescence scanner. This versatile method of protein analysis can be performed on almost any protein with a known antibody.

Initial western blot results of MC3T3 cells show a relative increase in TREK-1 expression in the cells grown on fiber surfaces compared to flat polymer surfaces. This can be seen in Figures 7&8. This indicates that mouse preosteoblasts grown on nanofiber surfaces would more readily express TREK-1, and possibly other potassium ion channels. Since the nanofiber architecture is more similar to the natural extracellular matrix than the flat control surfaces, this may show that TREK-1 expression in down regulated on flat surfaces.

When the same method was attempted with MG63 and hMSC cells, mixed results were obtained (Figures 11-13). While this may be that extracellular architecture has little effect on

human osteoblast and mesenchymal cells, it is also possible that the mixed results are due to the concentrations of the protein within the cell. When performing the western blot, four times the concentration of antibody was required to visualize the TREK-1 bands. This indicates that the ion channel exists at low concentrations within the cell, making it difficult to accurately analyze with conventional protein imaging and analysis methods. It is also believed that low concentrations of cells existed in the samples, making the free TREK-1 in the lysate low in concentration. In order to provide a more accurate quantitative analysis of the expression trend, an ELISA was performed.

4.4 ELISA and PicoGreen Assay

ELISA's and protein assays are often used to quantify the concentrations of their target protein within a sample lysate. These experimental methods are much more accurate at quantifying protein levels than traditional western blotting. Elisa's work by binding the target protein to the dish wall through the use of antibodies. Next, another antibody binds to the protein, followed by a third antibody binding to the second. When the second and third antibody are bound together, they will exhibit a specific absorbance of a wavelength of light that can be measured. A standard, an array of lysates with known protein concentration, is used to determine the relation between emission levels and concentration of protein. This reliable method has many variations and is used to quantify the expression of protein levels to a high degree of accuracy.

The ELISA for TREK-1 was normalized to double stranded DNA (dsDNA) to account for variations in cell numbers. The PicoGreen assay measures the amount of double stranded DNA present in a lysate by an emission/excitation pattern. This can be used to determine the

relative number of cells using a standard curve with known dsDNA concentrations. The PicoGreen assay of hMSCs cultured on flat and fiber surfaces showed an increase in dsDNA on flat surfaces compared to fiber surfaces. This can be expected since the flat surfaces provide more area for cells to divide and grow, as seen in Figure 14 and therefore create more dsDNA.

Raw ELISA values were inconclusive due to a high control sample compared to test sample. During data processing, this would have resulted in a negative TREK-1 concentration, which would be physically impossible. These low ELISA values most likely stem from two causes, similar to the problems experienced during western blotting. Low cell counts in the lysate can make it difficult for the ELISA to accurately read the levels of protein. This issue, compounded by low cellular concentrations of protein, make TREK-1 a difficult protein to images and analyze.

But if the blank/control values are not subtracted from the samples, a slight pattern can be observed. Compared to other surfaces, fibers with a diameter of 300nm appear to show a slight increase in TREK-1 expression, which can be observed in Figure 17 with statistical significance. Additionally, a larger trend can be seen when the ELISA is performed on hMSCs grown on larger diameter fibers. It appears that TREK-1 is more prone to increase expression on fibers of smaller diameter than those of a larger diameter, but statistical significance was not achieved. While this data cannot be viewed as reliable due to the lack of normalization the background, it does show that there may be an inverse trend in TREK-1 expression compared to nanofiber size. It may also show a decrease in the expression of TREK-1 on flat surfaces, similar to the western blot results. Since the nanofiber matrix is more similar to the natural ECM, this may indicate that TREK-1 expression is down regulated on flat surfaces.

4.5 Conclusions and Future Directions

Regenerative medicine through synthetic nanofiber extracellular matrices will continue to require years of effort in order to perfect techniques needed in for many clinical uses. But the potential benefits of these designs allow for many efforts to be justified. By designing artificial tissue scaffolds that intuitively instruct cells to grow and differentiate along a desired pathway, we can eliminate the need for auto- and allografts, reducing complication rates and increasing quality of life.

While this investigation was inconclusive due to low concentration of the target protein, there is some evidence that osteoblasts and hMSCs cultured on fibers surfaces alter their expression of TREK-1. Future work in this area would require increased cell concentrations, in addition to a wider variety of fiber shapes and architectures. The effects of fiber orientation were not studied in this investigation, but that parameter may have an effect on the expression of many transmembrane channels. Other areas to consider are how extracellular architecture will affect the cell membrane potential by changing the expression levels of TREK-1.

Continued work in this area will only increase our understanding of how cells are impacted by the physical surroundings and what they do in response to changes in these extracellular geometries. By increasing our understanding, we can someday hope to utilize cells and materials to increase the quality of living for patients in need.

BIBLIOGRAPHY

1. Stevens MM. Biomaterials for bone tissue engineering. *Mater Today*. 2008;11(5):18-25. doi:10.1016/S1369-7021(08)70086-5.
2. Salgado AJ, Coutinho OP, Reis RL. Bone tissue engineering: State of the art and future trends. *Macromol Biosci*. 2004;4(8):743-765. doi:10.1002/mabi.200400026.
3. Brydone AS, Meek D, Maclaine S. Bone grafting, orthopaedic biomaterials, and the clinical need for bone engineering. *Proc Inst Mech Eng Part H J Eng Med*. 2010;224(12):1329-1343. doi:10.1243/09544119JEIM770.
4. Clarke B. Normal bone anatomy and physiology. *Clin J Am Soc Nephrol*. 2008;3 Suppl 3. doi:10.2215/CJN.04151206.
5. Rho JY, Kuhn-Spearing L, Zioupos P. Mechanical properties and the hierarchical structure of bone. *Med Eng Phys*. 1998;20(2):92-102. doi:10.1016/S1350-4533(98)00007-1.
6. Carano RAD, Filvaroff EH. Angiogenesis and bone repair. *Drug Discov Today*. 2003;8(21):980-989. doi:10.1016/S1359-6446(03)02866-6.
7. Brighton CT, Hunt RM. Early histologic and ultrastructural changes in microvessels of periosteal callus. *J Orthop Trauma*. 1997;11(4):244-253. doi:10.1097/00005131-199705000-00002.
8. O'Keefe RJ, Mao J. Bone Tissue Engineering and Regeneration: From Discovery to the Clinic—An Overview. *Tissue Eng Part B Rev*. 2011;17(6):389-392. doi:10.1089/ten.teb.2011.0475.
9. Burg KJ., Porter S, Kellam JF. Biomaterial developments for bone tissue engineering.

Biomaterials. 2000;21(23):2347-2359. doi:10.1016/S0142-9612(00)00102-2.

10. Moore WR, Graves SE, Bain GI. Synthetic bone graft substitutes. *ANZ J Surg*. 2001;71(6):354-361. doi:10.1046/j.1440-1622.2001.02128.x.
11. Damien CJ, Parsons JR. Bone graft and bone graft substitutes: a review of current technology and applications. *J Appl Biomater*. 1991;2:187-208. doi:10.1002/jab.770020307.
12. Kumar G, Narayan B. Morbidity at bone graft donor sites. In: *Classic Papers in Orthopaedics*. ; 2014:503-505. doi:10.1007/978-1-4471-5451-8_132.
13. Mankin HJ, Gebhardt MC, Jennings LC, Springfield DS, Tomford WW. Long-term results of allograft replacement in the management of bone tumors. *Clin Orthop Relat Res*. 1996;324(324):86-97. doi:10.1097/01241398-199609000-00082.
14. Liu X, Ma PX. Polymeric scaffolds for bone tissue engineering. *Ann Biomed Eng*. 2004;32(3):477-486. doi:10.1023/B:ABME.0000017544.36001.8e.
15. Rezwan K, Chen QZ, Blaker JJ, Boccaccini AR. Biodegradable and bioactive porous polymer/inorganic composite scaffolds for bone tissue engineering. *Biomaterials*. 2006;27(18):3413-3431. doi:10.1016/j.biomaterials.2006.01.039.
16. Dhandayuthapani B, Yoshida Y, Maekawa T, Kumar DS. Polymeric scaffolds in tissue engineering application: A review. *Int J Polym Sci*. 2011;2011. doi:10.1155/2011/290602.
17. Gunatillake PA, Adhikari R, Gadegaard N. Biodegradable synthetic polymers for tissue engineering. *Eur Cells Mater*. 2003;5:1-16. doi:10.22203/eCM.v005a01.
18. Pham QP, Sharma U, Mikos AG. Electrospinning of Polymeric Nanofibers for Tissue Engineering Applications: A Review. *Tissue Eng*. 2006;12(5):1197-1211. doi:10.1089/ten.2006.12.1197.

19. Huang ZM, Zhang YZ, Kotaki M, Ramakrishna S. A review on polymer nanofibers by electrospinning and their applications in nanocomposites. *Compos Sci Technol*. 2003;63(15):2223-2253. doi:10.1016/S0266-3538(03)00178-7.

20. Cui W, Zhou Y, Chang J. Electrospun nanofibrous materials for tissue engineering and drug delivery. *Sci Technol Adv Mater*. 2010;11(1):14108. doi:10.1088/1468-6996/11/1/014108.

21. Yoo HS, Kim TG, Park TG. Surface-functionalized electrospun nanofibers for tissue engineering and drug delivery. *Adv Drug Deliv Rev*. 2009;61(12):1033-1042. doi:10.1016/j.addr.2009.07.007.

22. Nisbet DR, Forsythe JS, Shen W, Finkelstein DI, Horne MK. Review paper: a review of the cellular response on electrospun nanofibers for tissue engineering. *J Biomater Appl*. 2009;24(1):7-29. doi:10.1177/0885328208099086.

23. Shafiee A, Soleimani M, Chamheidari GA, et al. Electrospun nanofiber-based regeneration of cartilage enhanced by mesenchymal stem cells. *J Biomed Mater Res - Part A*. 2011;99 A(3):467-478. doi:10.1002/jbm.a.33206.

24. Ruckh TT, Kumar K, Kipper MJ, Popat KC. Osteogenic differentiation of bone marrow stromal cells on poly(??-caprolactone) nanofiber scaffolds. *Acta Biomater*. 2010;6(8):2949-2959. doi:10.1016/j.actbio.2010.02.006.

25. Chiquet M, Gelman L, Lutz R, Maier S. From mechanotransduction to extracellular matrix gene expression in fibroblasts. *Biochim Biophys Acta*. 2009;1793(5):911-920. doi:10.1016/j.bbamcr.2009.01.012.

26. Hughes S, Magnay J, Foreman M, Publicover SJ, Dobson JP, El Haj AJ. Expression of the mechanosensitive 2PK+ channel TREK-1 in human osteoblasts. *J Cell Physiol*.

2006;206(3):738-748. doi:10.1002/jcp.20536.

27. Bonewald LF, Johnson ML. Osteocytes, mechanosensing and Wnt signaling. *Bone*. 2008;42(4):606-615. doi:10.1016/j.bone.2007.12.224.

28. Papachroni KK, Karatzas DN, Papavassiliou KA, Basdra EK, Papavassiliou AG. Mechanotransduction in osteoblast regulation and bone disease. *Trends Mol Med*. 2009;15(5):208-216. doi:10.1016/j.molmed.2009.03.001.

29. Harada S, Rodan G a. Control of osteoblast function and regulation of bone mass. *Nature*. 2003;423(6937):349-355. doi:10.1038/nature01660.

30. Davidson RM, Tatakis DW, Auerbach AL. Multiple forms of mechanosensitive ion channels in osteoblast-like cells. *Pflügers Arch Eur J Physiol*. 1990;416(6):646-651. doi:10.1007/BF00370609.

31. Martinac B. Mechanosensitive ion channels: molecules of mechanotransduction. *J Cell Sci*. 2004;117(12):2449-2460. doi:10.1242/jcs.01232.

32. Rossi CA, Pozzobon M, De Coppi P. Advances in musculoskeletal tissue engineering. *Organogenesis*. 2010;6(3):167-172. doi:10.4161/org.6.3.12419.

ACADEMIC VITA

Academic Vita of Grant Wandling
gdw5051@psu.edu
717-275-5319

Education
Major: Biomedical Engineering
Honors: Biomedical Engineering

Thesis Title: The Role of Mechanically Gated Ion Channels in Regulating the Response to Nanofiber Architecture in Mesenchymal Stem Cells.
Thesis Supervisor: Justin L. Brown, Ph.D.

Work Experience
Date: June ‘17-August ‘17
Title: Undergraduate Researcher
Description: Investigated the correlations of basic body metrics and measurements to signs and symptoms of pre-clinical cardiomyopathy in pediatric obesity.
Institution/Company: Geisinger Medical Center, Danville, PA
Supervisor’s Name: Brandon Fornwalt M.D., Ph.D. & Christopher Haggerty, Ph.D.

Grants Received: Pinnacle Health Auxiliary Scholarship 2014-17

Awards: Dean’s List Fall ’14 – Fall ’17, Most Outstanding Poster in Clinical Sciences at the Susquehanna Valley Undergraduate Research Symposium.

Presentations: Susquehanna Valley Undergraduate Research Symposium

Community Service: Carlisle Emergency Department Volunteer 2015-16

Activities/Leadership: Penn State Men’s Water Polo Captain 2016-18, Penn State Women’s Water Polo Coach 2016-18